Evaluation of a New Jet Flap Propulsive-Lift System

Ya-Tung Chin*
Lockheed-Georgia Company, Marietta, Ga.

and

Thomas N. Aiken†
NASA Ames Research Center, Moffett Field, Calif.

and

Garland S. Oates, Jr.‡
Air Force Flight Dynamics Laboratory, Wright-Patterson Air Force Base, Ohio

A large-scale STOL transport model with an advanced internally blown jet flap (AIBF) was investigated in the NASA Ames 40- by 80-ft Wind Tunnel. Aerodynamically, the AIBF system combines the benefits of the jet flap and the mechanical flap with boundary-layer control. Structurally, it creates its own spanwise air duct with the deflection of the mechanical flap. An additional short-chord, fast-acting control flap located at the jet-flap exit provides a powerful means for flight-path and lateral controls. The results showed that the overall effectiveness of the AIBF compared well with other jet flap propulsive-lift systems. A preliminary design and performance study was made of a medium-size, turbofan-powered AIBF STOL transport for a typical military mission. This study showed that the AIBF results in a configuration with a relatively low T/W ratio, making the system an attractive candidate for future designs.

Nomenclature

b	= wing span, ft
c	= wing chord parallel to plane of symmetry, ft
$\bar{c}$, MAC	= mean aerodynamic chord, ft
C_D	= drag coefficient, drag $/qS$
C_J	= total isentropic jet thrust coefficient, T/qS
C_ℓ	= rolling-moment coefficient, rolling moment/qSb
C_L	= lift coefficient, lift/qS
$C_{L_{MAX}}$	= maximum value of the lift coefficient
$C_{L_{\alpha=0°}}$	= lift coefficient at 0° angle of attack
C_m	= pitching-moment coefficient about $0.262\bar{c}$, pitching moment/$qS\bar{c}$
C_n	= yawing-moment coefficient, yawing moment/qSb
i_t	= horizontal tail incidence, deg
q	= freestream dynamic pressure, psf
S	= wing area, ft^2
t	= wing thickness, ft
T	= total isentropic thrust of wing jets, lb
W	= gross weight, lb
WRP	= wing reference plane
α	= model angle of attack, deg
δ_c	= control-flap deflection, deg
δ_{cR}, δ_{cL}	= right and left control-flap deflection, deg
δ_f	= main-flap deflection, deg
Δ	= incremental change

Presented as Paper 74-993 at the AIAA 6th Aircraft Design, Flight Test and Operations Meeting, Los Angeles, California, August 12-14, 1974; submitted August 22, 1974; revision received December 5, 1974. This work was jointly sponsored by the NASA Ames Research Center, the U.S. Air Force Flight Dynamics Lab., and the Lockheed-Georgia Co.

Index categories: Aircraft Testing (Including Component Wind Tunnel Testing); Aircraft Aerodynamics (Including Component Aerodynamics).

*Scientist, Advanced Flight Sciences Department. Member AIAA.

†Aerospace Engineer, Large-Scale Aerodynamics Branch, Flight Systems Research Division.

‡Aerospace Engineer, Advanced Concepts Branch, Prototype Division. Member AIAA.

Introduction

A NEW generation of subsonic turbofan transport aircraft with takeoff and landing field lengths from 1500-2000 ft may eventually be required by the military and by the commercial airlines. For aircraft to attain such basic short takeoff and landing (STOL) performance, they must operate at takeoff and landing speeds substantially slower than those of today's jet transports. To reduce takeoff and landing speeds, the most effective method is to increase the maximum lift coefficient of the wing. The widely accepted approach is to integrate the propulsion and the high-lift systems so that propulsive thrust is used to augment aerodynamic lift during low-speed operation.

Since the jet flap is a very effective means to obtain efficient lift augmentation, most propulsive-lift systems proposed for

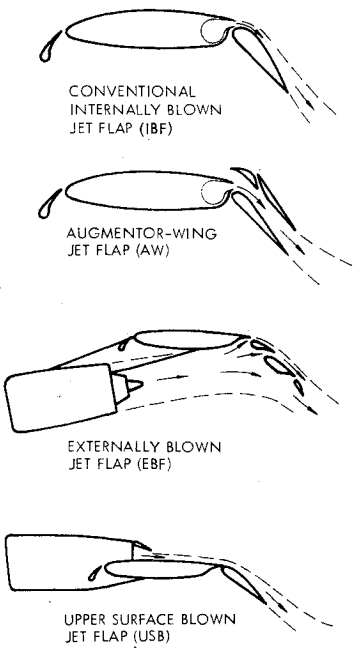

Fig. 1 Some jet-flap concepts.

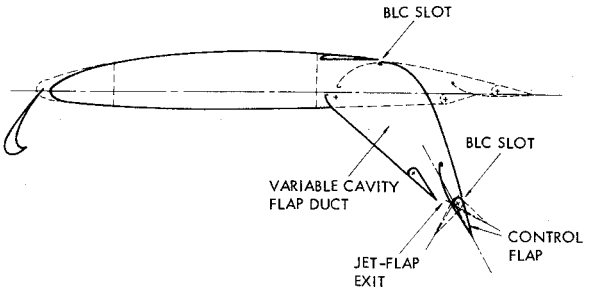

Fig. 2 Features of AIBF concept.

turbofan STOL aircraft are based on the jet-flap principle. These concepts invariably incorporate a mechanical flap to deflect, or turn, all or a portion of the installed engine thrust to create the jet-flap effect at the trailing edge. Some well-known jet-flap concepts are illustrated in Fig. 1. While all jet-flap concepts are capable of producing high lift coefficients, to integrate a design many other factors must be considered. The considerations include axial force characteristics, noise characteristics, low-speed handling qualities, engine-out safety, cruise performance, mechanical complexity, design flexibility, system weight, and economics.

Recently, an advanced internally blown jet flap (AIBF) concept was developed at the Lockheed-Georgia Co. As depicted in Fig. 2 in its basic configuration, this concept has a unique trailing-edge flap geometry which combines several features to produce a versatile propulsive-lift system. During low-speed flights, it also performs as an integral part of the basic flight-control system. A tripartite research on the AIBF using a large-scale STOL transport model for experimental investigation in the NASA Ames 40- by 80-ft Wind Tunnel was completed in 1973.[1,2] The AIBF is discussed here with respect to its aerodynamic characteristics and a preliminary design application.

New Jet-Flap Concept

The special aerodynamic feature of the AIBF concept is the simultaneous blowing from two primary spanwise slots. A small proportion of the total available air supply is blown from an upper boundary-layer control (BLC) slot to maintain flow attachment on the deflected main flap. For maximum efficiency, the main jet is discharged through a lower slot near the trailing edge in the pure jet-flap manner.

The outstanding structural feature of this concept is that it creates its own internal-flow duct system. During deflection of the main flap, the upper and lower flap elements move apart to create a spanwise cavity within the flap. The cross-section of this cavity enlarges with increasing flap deflections so that an air duct is provided for the distribution of large quantities of blowing air with low duct losses. This obviates the ducting-space problem usually encountered by internal-blowing systems.

Another unique feature of this concept is a short-chord, fast-acting control flap. Positioned in the proximity of the jet-flap exit, it provides an effective means for deflecting the jet flap for lift, drag, and lateral controls. BLC blowing is provided at the knee of the control flap to increase its effectiveness at large deflections.

Model Description

Figure 3 shows the general arrangement of the model used for the experimental investigation. Pertinent model reference data are presented in Table 1. The model wing had a full-span, non-optimum slat of 0.15 chord. The wing section and flap geometry were identical to that depicted in Fig. 2. The upper BLC slot and the jet-flap exit were located at 0.695 and 0.893 chord, respectively; adjustable vanes were provided to change these gaps. The fixed-gap aft BLC slot for the control flap was located at 0.925 chord. The flap system could be configured either as a full-span flap or with the outboard 30% span as a BLC aileron.

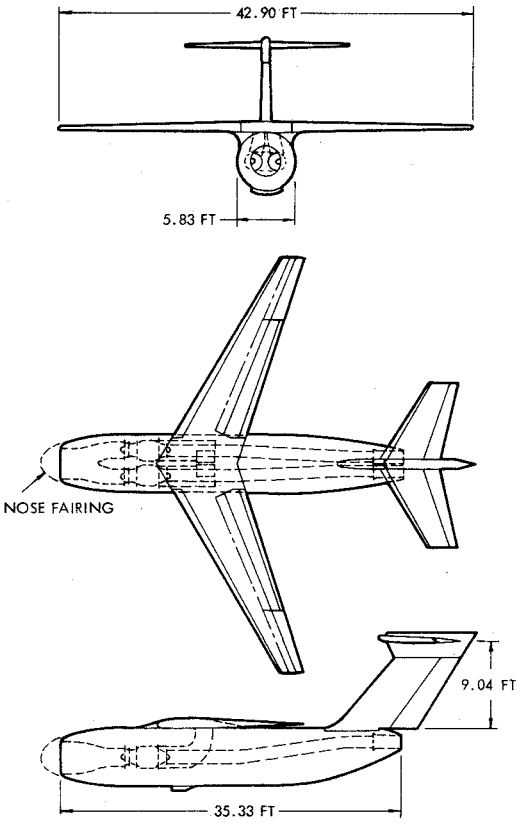

Fig. 3 Model general arrangement.

Table 1 Model reference data

Item	Wing	H. Tail	V. Tail
Area, sq ft	230.0	72.371	68.0
Aspect ratio	8.0	3.993	1.20
Taper ratio	0.30	0.490	0.74
Span, ft	42.895	17.00	9.042
Root chord, ft	8.250	5.714	8.645
Tip chord, ft	2.475	2.800	6.397
MAC, ft	5.881	4.423	7.577
Sweep ($c/4$), deg	27.5	25	38.5
Airfoil section	65A-4[a]	64-012[b]	0012
Tail arm, ft		20.10	17.36
Tail vol. coeff.		1.075	0.120

[a] $(t/c)_{root} = 0.125$, $(t/c)_{tip} = 0.105$. [b] Inverted.

Two Pratt & Whitney JT15D-1 turbofan engines were mounted in the fuselage. All the cold bypass air of each engine was ducted to the flap cavity of a wing to power the blowing slots. The hot gas from the core engine was exhausted out the tailpipe; noise suppressors were provided for the air inlet and tailpipes. A nose fairing was installed during part of the tests.

The vertical tail was on the model at all times. When the horizontal tail was installed, it was equipped with a 40° inverted slat of 0.15 tail chord. The elevator and rudder deflections were always set at 0°.

Test Program

Tests were made without and with the horizontal tail at wind-tunnel dynamic pressures corresponding to Reynolds numbers from 2-5.35 million, based on the wing mean aerodynamic chord, and at static conditions. Both full-span and part-span flap configurations were tested. Data were obtained for 30° and 60° main-flap deflections in combination with various control-flap deflections. These included six-

component data, flap-duct total pressures and temperatures, surface static pressures, noise data, and tail-off downwash data.

All final force and moment data were corrected for wind tunnel wall effects, inlet momentum drag, and tailpipe thrust. For data computation, the moment center was located at $0.262\bar{c}$ longitudinally and $0.20\bar{c}$ below the wing chord plane. The wing chord plane was 4.12 in. above the fuselage.

The isentropic jet thrust of each blowing slot was computed from the measured duct total pressures and temperatures and the slot areas. C_J is the sum of all the component thrust coefficients. It was estimated that the actual thrust was approximately 0.85 of the isentropic value.

Discussion of Results

Selected results of tests with 30° and 60° main flaps in combination with various control-flap deflections, in the part-span flap configuration, are presented for the discussion. The results were obtained with the BLC aileron drooped 30° and the slat deflected 60°. For the 30° flaps, the thrust contributions of the upper BLC slot, the aft BLC slot, the jet flap, and the aileron BLC slot were 7.0, 13.2, 74.2, and 5.6% of the total isentropic jet thrust, respectively. The corresponding values for the 60° flaps were 12.8, 13.2, 68.6, and 5.4%. The typical takeoff-flap setting was represented by a 30° flap with 0° control-flap deflection. A 60° flap with 20° control-flap deflection represented the typical landing-flap setting. With the horizontal tail installed, the tail incidence was set at -15° and -10° for the typical takeoff and landing flaps, respectively.

The tail-on lift and drag results for the typical takeoff and landing flaps are shown in Figs. 4 and 5, respectively. Superimposed on the drag polars of these figures are constant flight-path lines and lines of constant T/W. The data clearly indicate the lift generating capability and STOL performance of the AIBF. For example, the landing flap produced a maximum lift coefficient of 8.15 at a thrust coefficient of 1.59. At a typical landing lift coefficient of 4.5, a descent angle of 9.8° can be provided at a thrust coefficient of 0.52 $(T/W = 0.116)$ and 5° angle of attack.

It is of interest to compare the lift performance of the various jet-flap concepts. To provide nearly uniform comparisons, recent data of large-scale tests of the AW,[3] IBF,[4] EBF,[5] and USB[6] were compared with the AIBF test results for a 60° flap with 0° control-flap deflection. The comparisons, in terms of the lift coefficients at 0° angle of attack and the maximum lift coefficients for a range of thrust coefficients, are shown in Fig. 6. It is seen that the effectiveness of the AIBF compares well with the other systems.

The lift and drag increments due to symmetric control-flap deflections and power are shown in Figs. 7 and 8 for 30° and 60° flaps, respectively. Up to a total jet-flap deflection of approximately 90° (the total of main-flap and control-flap deflections), these increments increased almost linearly with control-flap deflections at constant thrust coefficients. Further forward deflection of the control flap provided additional drag increase, but with little lift change. This indicates that the control flap could be used to increase lift and drag without the need for high main-flap deflections. It also permits the effective control of the landing lift-to-drag ratio to achieve prescribed flight paths.

In Fig. 9, test data show that for typical takeoff- and landing-flap settings, the addition of power to both the tail-off and tail-on configurations produced stable pitching moments. The constant tail contribution to pitching moments indicated that the downwash at the horizontal tail was relatively constant above a thrust coefficient of approximately 0.4 for both flap settings, and trim capability should not be a problem.

The rolling and yawing moment increments due to asymmetric control-flap deflections and power are shown in Fig. 10 for a 30° flap and a typical takeoff lift coefficient of 3.5. At constant power, the rolling moment increments increased

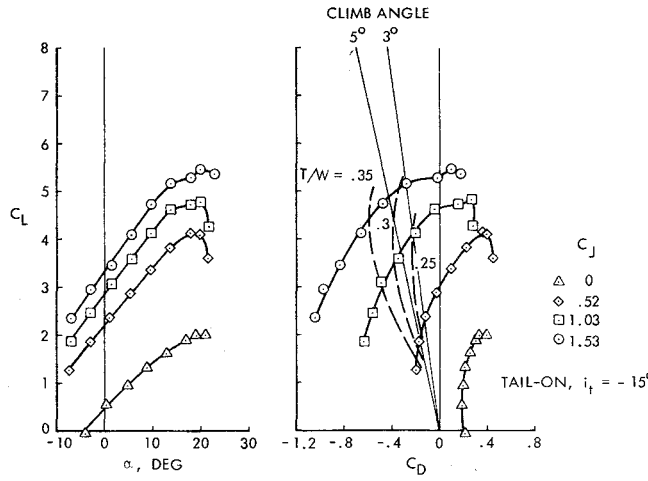

Fig. 4 Longitudinal characteristics-$\delta_f = 30°$, $\delta_c = 0°$.

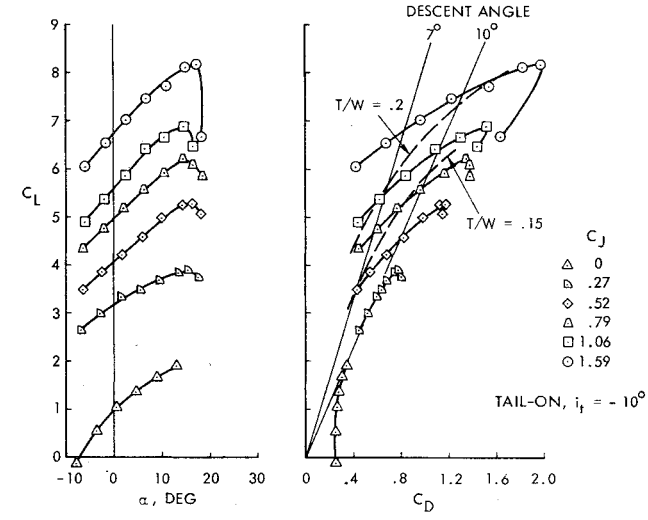

Fig. 5 Longitudinal characteristics-$\delta_f = 60°$, $\delta_c = 20°$.

linearly with control-flap deflections. For a roll-control gearing of -20° and 40°, at a thrust coefficient of 1.5, the total roll coefficient was apparently sufficient to produce good roll performance. Although asymmetric control flaps also produced adverse yawing moments, the level of directional control determined by the engine-out and cross-wind considerations should be more than adequate to accomplish turn coordination during abrupt maneuvers.

Figure 11 is similar to Fig. 10, except that it is for a 60° flap and a typical landing lift coefficient of 4.5. At constant power, the rolling moment also increased linearly with control-flap deflections, but the increments were slightly lower than for the 30° flap. The total adverse yawing moments did not appear to be increased by the higher flap deflection.

Design Application

A preliminary design application study was made of a typical military AIBF STOL transport to establish design and performance data. The design mission requirements and basic ground rules are shown in Table 2. For computing STOL takeoff and landing performance, the aerodynamic data from the large-scale tests were used.

Figure 12 shows the configuration and geometric characteristics of the study airplane, which has an operating weight empty of 114,200 lb and a 2.5g ramp weight of 204,000 lb. Conventional structural design was used for the fuselage, empennage, and wing. A supercritical airfoil section was selected for the wing, as it resulted in lower cost and weight than a conventional section. The wing has 70%-span AIBF flaps of

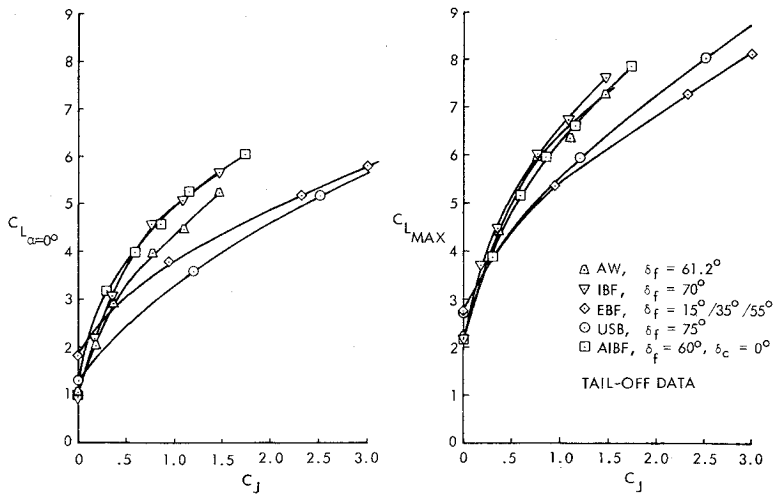

Fig. 6 Lift performance comparisons.

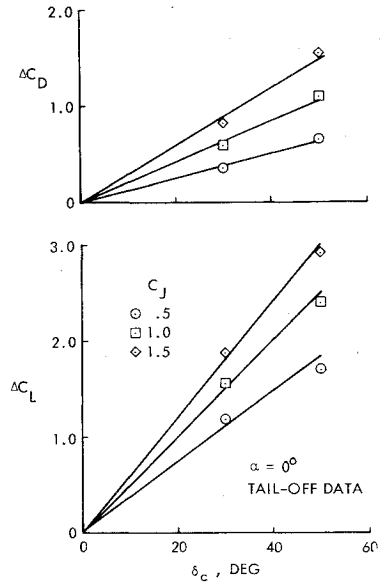

Fig. 7 Effect of symmetric control-flap deflections on lift and drag, $\delta_f = 30^\circ$.

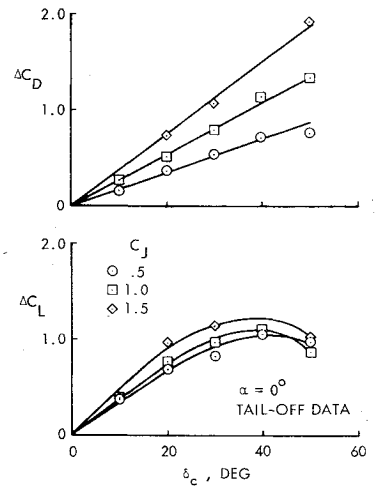

Fig. 8 Effect of symmetric control-flap deflections on lift and drag, $\delta_f = 60^\circ$.

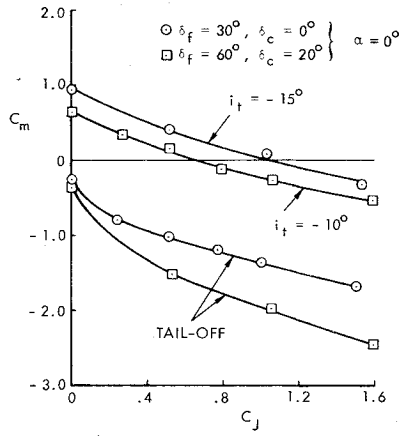

Fig. 9 Trim shift due to power.

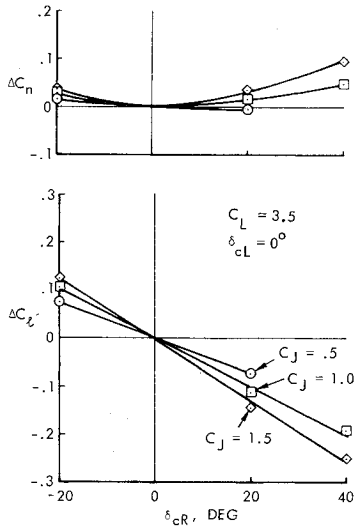

Fig. 10 Effect of asymmetric control-flap deflections on rolling and yawing moments, $\delta_f = 30^\circ$.

0.30 chord and slats of 0.17 chord. Takeoff-flap setting is 30° main flap with 0° control-flap deflection. Landing-flap setting is 30° main flap with 50° control-flap deflection. The AIBF flaps were assumed to be no heavier than EBF flaps of a similar airplane and were approximately 15 lb/ft^2. Sufficient fuel volume to fly the required 3700-naut miles ferry range is provided by the complete wing box.

For the study airplane, the engine used was a Pratt & Whitney STF402-AT. The sea level static thrust of this engine is 21,800 lb flat rated to 103°F. The bypass ratio is 5.0, and the fan pressure ratio is 1.57. Figure 13 shows the engine installation. During the takeoff and landing modes, all the cold bypass air is collected via a transition duct and exhausted above, and slightly aft, of the primary-exhaust exit. The bypass-air exit area was sized for transfer of low-velocity fan air (Mach 0.35-0.40) into an identically sized opening in the lower skin of the AIBF flap for powering the slots. For midpoint takeoff, the bypass air provides a thrust coefficient of approximately 0.94. At 35% power, it provides a thrust coefficient of approximately 0.32 for midpoint landing. To minimize exhaust interference with the jet flap, the primary exhaust is deflected 10° downward at the nozzle.

In addition, when the flaps are retracted for cruise, the bypass-air exit nozzle is contracted by lowering a door hinged

to the upper wall of the transition duct. This provides the necessary reduction in exit area to increase the velocity of the fan air to match cruise efficiency. Actuation of this door deflects the bypass-air exhaust away from the bottom skin of the flaps behind each engine to avoid scrubbing drag. It also opens an exit for the passage of ram air entering through blow-in doors located in the leading edge of the pylon structure. This eliminates the base-drag penalty behind the large flat-plate bypass exit.

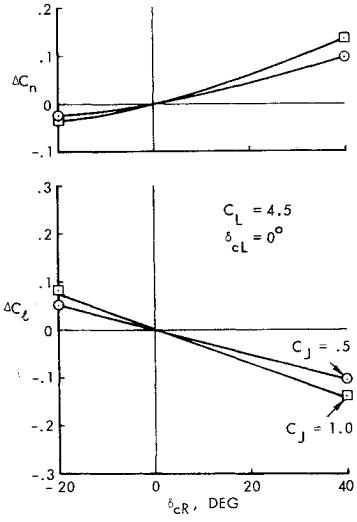

Fig. 11 Effect of asymmetric control-flap deflections on rolling and yawing moments, $\delta_f = 60°$.

Table 2 Design constraints

Employment mission	
payload (3.0g, 500 naut miles radius)	28,000 lb
radius	500 naut miles
field length (2500 ft 93°F)	2000 ft
climb angle	3°
approach angle	7.5°
runway surface (CBR)	6
penetration speed at 1000 ft	350 knots
airdrop speed range	100-200 knots
Deployment mission	
payload (2.5g, 1000 naut miles range)	58,000 lb
ferry range	3700 naut miles
cruise Mach (long range)	0.75
Cargo compartment	
width	11.7 ft
height	12 ft
length	55 ft

Performance of AIBF-STOL

The performance summary of the study airplane is presented in Table 3. For this study, the airplane was essentially sized for the payload range and the ferry range of the deployment mission. Even though this mission did not fully exploit the high-lift potential of the AIBF, the results reveal that this system can yield an airplane with performance characteristics which compare favorably with other propulsive-lift systems. The thrust-to-weight ratio of 0.394, for instance, is low enough to identify the AIBF as an attractive contender in future STOL designs.

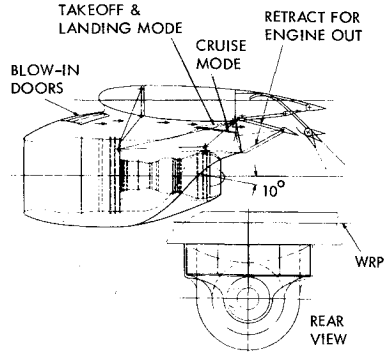

Fig. 12 AIBF-STOL general arrangement.

Table 3 Performance summary

Employment mission	
payload (3.0g, 500 naut miles radius)	28,000 lb
cruise speed	0.75 Mach
midpoint weight	160,000 lb
wing loading	72.8 lb/ft^2
installed thrust/weight	0.394
midpoint takeoff (2500 ft 93°F)	
distance over 50 ft	1950 ft
ground roll	1340 ft
lift-off speed	88 ktas
engine-out climb angle	5.8°
midpoint landing (2500 ft 93°F)	
distance over 50 ft	1920 ft
ground roll	1400 ft
approach speed	89 ktas
approach rate-of-sink	1180 ft/min
Deployment mission	
payload (2.5g, 1000 naut miles range)	58,000 lb
ferry range	3700 naut miles
cruise speed (long range)	0.75 Mach

	WING	H. TAIL	V. TAIL
AREA SQ.FT.	2180	427	485
ASPECT RATIO	7.0	5.25	1.24
TAPER RATIO	0.4	0.4	0.6
SPAN FT.	123.5	47.3	24.5
MAC FT.	18.7	9.6	20.2
SWEEP (c/4)	10°22'	13°46'	35°

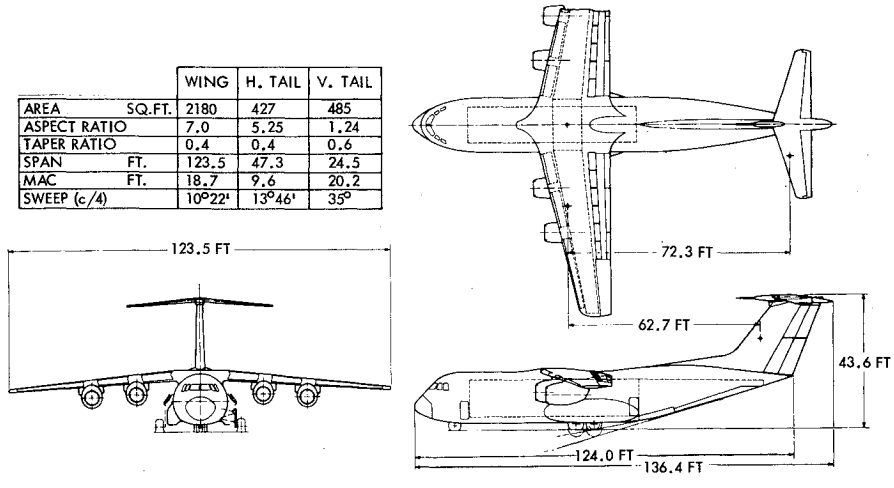

Fig. 13 AIBF- STOL engine installation.

Conclusions

The results of an experimental and preliminary design evaluation of the AIBF propulsive-lift system have been presented. The data show that the AIBF has excellent lift- and control-augmentation capability and is a strongly competitive system. Other factors being equal, at least two aspects of this system make it quite attractive for consideration in future designs. One is the versatility provided by the short-chord control flap. Articulating the control flap for fast jet deflections provides effective direct-lift and lateral controls which are very desirable in the STOL environment. The availability of the control flap also offers the possibility of using one main-flap deflection for both takeoff and landing. Another attractive feature of the AIBF is that the expandable flap-duct concept permits lower duct and exit velocities. In turn, this represents the potential for lower operating noise levels of jet-flap STOL aircraft.

References

[1]O'Lone, R. G., ,'Wide Range of Applications Seen for High-Lift System," *Aviation Week and Space Technology,* Vol. 98, No. 6, Feb. 5, 1973, p. 61.

[2]Aiken, T. N., Aoyagi, K., and Falarski, M. D., "Aerodynamic Characteristics of a Large-Scale Model with a Swept Wing and a Jet Flap Having an Expandable Duct," TM X-62,281, Sept. 1973, NASA.

[3]Falarski, M. D. and Koenig, D. G., "Aerodynamic Characteristics of a Large-Scale Model with a Swept Wing and Augmented Jet Flap," TM X-62,029, July 1971, NASA.

[4]Falarski, M. D. and Koenig, D. G., "Longitudinal and Lateral Stability and Control Characteristics of a Large-Scale Model with a Swept Wing and Augmented Jet Flap," TM X-62,145, April 1972, NASA.

[5]Aoyagi, K., Falarski, M. D., and Koenig, D. G., "Wind Tunnel Investigation of a Large-Scale 25° Swept-Wing Jet Transport Model with an External Blowing Triple-Slotted Flap," TM X-62,197, Nov. 1973, NASA.

[6]Aoyagi, K., Falarski, M. D., and Koenig, D. G., "Wind Tunnel Investigation of a Large-Scale Upper Surface Blown-Flap Transport Model Having Two Engines," TM X-62,296, Aug. 1973, NASA.